# Scd1 diffuses end to end along the cytoplasm to facilitate Cdc42 activation and bipolar growth

**Marcus A Harrell, Olivia Chinsen, Maitreyi Das[§]**

Biology Department, Boston College, Chestnut Hill, MA, 02467

[§] **Corresponding author:** Maitreyi.Das@bc.edu

**Running title:** Scd1 diffusion drives bipolar growth

**Word count:**

**ABSTRACT**

The conserved GTPase Cdc42 is a major regulator of polarized growth in most eukaryotes. In *Schizosaccharomyces pombe*, Cdc42 activity displays anticorrelated oscillatory dynamics between the growing ends enabling bipolarity. Cdc42 at each end is activated only when the opposite end loses activity. This suggests that a regulator of Cdc42 likely travels end-to-end to activate Cdc42. The oscillatory dynamics between the growing ends have also been observed in Cdc42 activator Scd1, its scaffold Scd2. It is unclear how these proteins move between the ends to facilitate bipolarity. We find that Scd1 does not travel between the cell ends via actin-mediated delivery. Instead, we show that Scd1 is mostly cytoplasmic and diffuses between the cell ends. The rate of diffusion is not entirely proportional to increasing the mass of Scd1 and cells lacking the inhibitor Pak1 kinase show decreased diffusion. Moreover, we show that Scd1 diffuses at a much faster rate compared to its scaffold Scd2. These findings suggest that Scd1 diffusion is not random and is regulated by Pak1 kinase. We find that decreasing the rate of diffusion disrupts Cdc42 oscillatory dynamics and results in monopolarity. Our results show that end-to-end Scd1 diffusion drives Cdc42 oscillatory dynamics and regulates cell polarity.

28 **SIGNIFICANCE STATEMENT.**

29 - Cdc42 activation shows oscillatory dynamics between the sites of growth
30 - The Cdc42 GEF Scd1 diffuses from site of activation to the opposite end to facilitate
31 these oscillatory dynamics
32 - This diffusion is not random and likely depends on intrinsic properties of the Scd1
33 protein.

34

35 **Keywords:** Cdc42, oscillations, Scd1, diffusion, Pak1 kinase, cell polarity

36 **INTRODUCTION**

37 The Rho Family GTPase Cdc42 is a major regulator of polarized growth across most
38 eukaryotes (Miller and Johnson, 1994; Johnson, 1999). Cdc42 is a molecular switch that is
39 active when GTP bound, and inactivated when GTP is hydrolyzed to GDP (Johnson,
40 1999). Active Cdc42 promotes F-actin polymerization and membrane trafficking for cell growth.
41 Thus, Cdc42 activity must be precisely coordinated among multiple sites of growth for proper
42 cell polarity and function (Nobes and Hall, 1999; Stengel and Zheng, 2011; Das and Verde,
43 2013). GTPases are activated by GEFs (Guanine nucleotide exchange factors) and inactivated
44 by GAPs (GTPase activating proteins) (Hall, 1990). GEFs activate Cdc42 by exchanging GDP
45 for GTP, while GAPs complete a catalytic triad to promote hydrolysis of GTP into GDP (Zhang
46 *et al.*, 1999; Scheffzek and Ahmadian, 2005).

47 The fission yeast *S. pombe* has a streamlined proteome compared to more complex
48 model systems. Cdc42 has around 20 GEFs and GAPs in mammalian cells (Rossman *et al.*,
49 2005). But, in *S. pombe*, there are only two Cdc42 GEFs, Scd1 and Gef1, and three Cdc42
50 GAPs (Murray and Johnson, 2001; Coll *et al.*, 2003). These streamlined signaling pathways
51 make *S. pombe* an excellent model to investigate Cdc42 regulation. *S. pombe* has 3 major
52 players for Cdc42 activation and growth, Gef1, Scd1, and the scaffold Scd2 (Chang *et al.*, 1994;
53 Sawin and Nurse, 1998; Chang *et al.*, 1999; Wheatley and Rittinger, 2005). The initial activation
54 of Cdc42 is mediated by Ras GTPase or Gef1 (Chang *et al.*, 1994; Hercyk *et al.*, 2019b). When
55 active, GTP-bound Cdc42 recruits Scd2 (Bem1p) to tether Scd1 (Cdc24p) to the membrane and
56 activate more Cdc42 (Butty *et al.*, 2002; Wheatley and Rittinger, 2005; Rapali *et al.*, 2017). This
57 results in a positive-feedback loop wherein Cdc42 activation is self-amplified (Butty, 2002;
58 Kozubowski *et al.*, 2008; Das and Verde, 2013).

59 During interphase, Cdc42 activity oscillates between the two growing ends (Das *et al.*,
60 2012). Cdc42 oscillations are anti-correlated, such that as one end gains Cdc42 activity, the

61 other end loses activation (Das *et al.*, 2012). This spatiotemporal patterning suggests that the
62 two ends are interconnected by some protein(s) that are alternately recruited to the growing
63 ends for oscillatory activation of Cdc42.

64 The identity of this factor or how it travels from one end to the other is unknown but
65 Cdc42 GEFs are a likely candidate. Previous work has shown Gef1 and Scd1 play distinct roles
66 in cytokinesis and Gef1 is a secondary GEF for Cdc42 activation and initiates growth at new
67 sites but is not the major GEF needed for polarized growth (Wei *et al.*, 2016; Hercyk *et al.*,
68 2019a). Indeed, *gef1*Δ mutants are mostly monopolar, but still polarized whereas *scd1*Δ mutants
69 are depolarized, and show spherical morphology (Hercyk *et al.*, 2019a). This suggests that
70 Scd1 is the primary GEF for cell polarity. Cdc42 oscillatory dynamics occur due to time-delayed
71 negative feedback where the Pak1 kinase prevents Scd1 recruitment to the cell membrane (Das
72 *et al.*, 2012). We have recently shown Scd1 returns to each cell end after inhibition by Pak1
73 kinase in an endocytosis-dependent manner. Pak1 kinase at each end is removed during
74 endocytosis and this allows the return of Scd1 for the next cycle of Cdc42 activation at that end
75 (Harrell *et al.*, 2024). We asked if the population of Scd1 within the cell sequentially moves from
76 one end to the other for oscillatory Cdc42 activation.

77 To this end, we used *in vivo* experiments in *S. pombe* to test if Scd1 travels from one
78 end to the other to promote bipolar growth. We find that in fission yeast, Scd1 is mostly
79 cytoplasmic and its localization to the ends is not dependent on actin-mediated delivery. Our
80 data shows that Scd1 diffuses between the two halves of the cell. Furthermore, Pak1 kinase
81 promotes faster diffusion of Scd1 within the cell. We show that Scd2 also localizes via
82 cytoplasmic diffusion, yet Scd1 molecules have a faster turnover between the two halves of the
83 cell and their growing ends when compared to Scd2 despite Scd2 being a smaller and more
84 abundant protein. Our data also show that simply increasing the mass of Scd1 does not linearly
85 decrease its diffusion dynamics even though it impacts its ability to promote bipolarity. Cells with

86 slower Scd1 diffusion show disrupted Cdc42 oscillatory dynamics and increased monopolarity.
87 Together, our findings here show that Scd1 diffuses from one end of the cell to the other to
88 promote oscillatory behavior but this does not occur via simple random diffusion and likely
89 depends on the properties and regulation of Scd1.

90 **RESULTS & DISCUSSION**

91 **Scd1 is highly cytoplasmic and diffuses between cell ends**

92 It is unknown how Scd1 is delivered to the cell ends for activation of Cdc42. We asked if
93 Scd1 localizes to the cell ends via membrane trafficking. We and others previously reported that
94 Scd1 localization is diminished at cell ends upon depolymerization of all F-actin during LatA
95 treatment (Hercyk *et al.*, 2019a; Salat-Canela *et al.*, 2021). Thus, we asked if Scd1 was
96 delivered via actin cables. We used *for3*Δ mutants, which cannot polymerize linear actin cables
97 for actin-mediated delivery during interphase (Feierbach and Chang, 2001; Nakano *et al.*, 2002;
98 Martin and Chang, 2006). We compared Scd1-mNG localization in *for3*$^{+}$ cells and *for3*Δ mutants
99 and found that Scd1 localization is not decreased by the lack of actin-mediated delivery (Fig.
100 1A, B). Together, these data suggest that Scd1 is not localized by actin-mediated membrane
101 trafficking. Furthermore, bipolar *for3*Δ mutants show increased Scd1 localization and
102 anticorrelated Cdc42 oscillations thus suggesting that actin does not facilitate delivery of Scd1.

103 Many yeast proteins localize in the cytoplasm as part of their function (Matsuyama *et al.*,
104 2006). Fluorescent microscopy of Scd1 shows high cytoplasmic fluorescence intensity relative
105 to the cell ends (Fig. 1A). We quantified the distribution of Scd1-mNG intensity throughout the
106 cell and find that Scd1 localization within the cytoplasm is high even when compared to the
107 more intense cell end (Fig. 1C). To quantify this metric, we averaged the intensity of the
108 cytoplasm and compared the cytoplasmic intensity to the two cell ends and found that the
109 cytoplasmic intensity of Scd1-mNG is about 50% of the total Scd1-mNG localized at the cell
110 ends (Fig. 1D). This suggests that there is a high ratio of Scd1-mNG that is localized in the
111 cytoplasm of the cell despite the low abundance of Scd1.

112 It has been established that the diffusion of solutes and macromolecules is important for
113 several cellular processes (Verkman, 2002). Due to high levels of Scd1-mNG in the cytoplasm
114 and Scd1-mNG localization occurring independent of membrane trafficking, we hypothesized

115 that Scd1-mNG localizes to cell ends via diffusion. To test this, we used fluorescence loss in
116 photobleaching (FLIP) (Cole *et al.*, 1996; White and Stelzer, 1999; Shcheprova *et al.*, 2008).
117 FLIP is a photomanipulation technique that measures the rate of protein exchange between two
118 regions of interest within a cell by repeatedly bleaching one area of the cell while measuring the
119 rate of fluorescence loss at a second region of interest within the cell. If fluorescence is lost at
120 the second region, this suggests that the two regions of interest exchange proteins (White and
121 Stelzer, 1999). Further, the rate of this loss can be used to approximate the rate of protein
122 exchange between these regions (Fig. 1E, top). If there is no exchange between the two regions
123 of interest, no loss in fluorescence will be observable at the second site (Fig. 1E, bottom).
124 We used FLIP to test if Scd1 is exchanged between the two ends of bipolar cells or if
125 each end has a distinct pool of Scd1. We bleached within the cytoplasm to ensure consistent
126 photobleaching for each experiment and fluorescence loss was observed at the cell end of the
127 opposite half of the cell from where cytoplasmic beaching occurs (Fig. 1F). We performed FLIP
128 on Scd1-mNG cells and found that the two halves of the cell do exchange Scd1-mNG, as one
129 half's cytoplasm is bleached, the growing end of the opposite half steadily loses fluorescence
130 above the rate of photobleaching (Fig. 1F and Fig. S2A). Notably, the low signal-to-noise ratio of
131 Scd1-mNG combined with photobleaching correction, results in a plateau of intensity when all
132 fluorescence has been lost (Fig. 1F, G). We found that the average time to lose 50%
133 fluorescence intensity from the opposing cell end was around 75 seconds (Fig. 1H). These
134 findings suggest that Scd1 is exchanged between the two halves of the cell and that Scd1 may
135 localize via diffusion.
136

137 **Increasing mass on Scd1 dampens Cdc42 activation and increases monopolarity**

138 We next asked if Scd1 dynamics can be dampened by increasing the mass on the
139 protein. Because Scd1 is the major activator of Cdc42, dampened Scd1 dynamics likely disrupts
140 proper Cdc42 activity. To test this, we observed CRIB-mCherry dynamics, which specifically
141 localize to the active form of Cdc42, in Scd1-mNG and Scd1-3xGFP strains (Fig. 2A). Scd1 is a
142 99.1kDa protein and each fluorophore adds roughly 26.6 kDa of mass. We tested Cdc42
143 activation dynamics in -mNG (+26.6 kDa) and -3xGFP strains (+79.8 kDa). Indeed, we find that
144 CRIB-mCherry oscillates between the two ends as expected in Scd1-mNG cells however CRIB-
145 mCherry dynamics are notably more monopolar in Scd1-3xGFP cells (Fig. 2A, B). To quantify
146 this difference, we measured how much CRIB-mCherry fluctuated between each time point at
147 the weaker cell ends and find that Cdc42 activation is less dynamic when Scd1 is massive as
148 seen with CRIB-mCherry in Scd1-3xGFP expressing cells (Fig. 2C).

149 To test the impact of adding additional mass to Scd1 on cell polarity, we stained cells
150 with calcofluor white to quantify the percentage of monopolar cells in cultures of cells with
151 fluorescently tagged Scd1. In addition to -mNG and -3xGFP, we also tested strains with -
152 tdTomato and -2xGFP (+54.2 kDa). We find there is an increased percentage of monopolar
153 cells as more mass is added to Scd1 suggesting that increased Scd1 mass dampens bipolar
154 Cdc4 activation and results in monopolar cells (Fig. 2D and Fig. S2A). In cells with increased
155 Scd1 mass a smaller but consistent fraction of the cells are bipolar, suggesting that it is rare but
156 still possible for Scd1 to accumulate at the opposite end. But under these conditions, this
157 evolutionary important system of bipolar growth no longer consistently functions within the
158 population (Fig. 2D).

159

160

161

162 **Increasing the mass on Scd1 does not proportionally decrease its diffusion dynamics**

163 Since Scd1 diffuses from one end of the cell to the other and increasing the mass of
164 Scd1 leads to increased monopolarity and altered Cdc42 activation patterns, we asked if Scd1
165 is distributed between ends via random diffusion in the cytoplasm. If this is true, the decrease in
166 Scd1 diffusion should be proportionally inverse to the increase in mass of this protein. We
167 aimed to test if Scd1 diffusion and localization to cell ends is slowed by adding more mass to
168 Scd1. We used FLIP to test if Scd1 diffusion was slower in populations that have more mass
169 added to Scd1 (Fig. 3A and Fig. S3A). We tested the rate of Scd1 loss in -mNG (+26.6 kDa), -
170 2xGFP (+53.2 kDa), and -3xGFP strains (+79.8 kDa) (Fig. 3B and Fig. S3A). We find that there
171 is a significant dampening of the rate of Scd1 loss in -2xGFP and -3xGFP strains when
172 compared to -mNG (Fig. 3C and Fig. S3A). While the half-life of Scd1-mNG fluorescence at the
173 cell end is still lost around 70 seconds, Scd1-2xGFP and Scd1-3xGFP cells show a half-life of
174 around 100 seconds. This suggests that additional mass does hinder Scd1 mobility and
175 dampens its dynamics. However, we did not see any change in the diffusion dynamics between
176 Scd1-2xGFP and Scd1-3xGFP. This indicates that in addition to mass other factors also
177 regulate Scd1 diffusion dynamics.

178 Next, we tested if Scd1 recruitment at the cell ends is perturbed by additional mass. To
179 this end, we used fluorescence recovery after photobleaching (FRAP) (Poo and Cone, 1974;
180 Axelrod *et al.*, 1976; Jacobson *et al.*, 1976). We bleached half of one cell end to standardize
181 the amount of bleaching and observe if the arrival of unbleached, new protein occurred via
182 lateral membrane diffusion or cytoplasmic diffusion (Fig. 3C). We observe that Scd1 recovery at
183 the photobleached region occurs without diminishing the intensity of the other half of the same
184 cell end which suggests that recovery occurs via the arrival of protein from the cytoplasm and
185 not due to the diffusion of the protein from one side of the end to the bleached side (Fig. S3B,
186 and Fig. S3C). Indeed, we found that Scd1 fluorescence recovery is significantly slower in -

187 2xGFP and -3xGFP strains when compared to Scd1-mNG (Fig. 3D, E). However, similar to our
188 FLIP data, we did not see any difference in the FRAP recovery of Scd1-2xGFP and Scd1-
189 3xGFP. This further suggests that Scd1 dynamics at the cell ends are only partially dependent
190 on its mass.

191 **Pak1 kinase facilitates Scd1 diffusion dynamics within the cell.**

192 In budding yeast, Cdc42 activates the PAK Kinase, Cla4 (Pak1), to phosphorylate and inhibit
193 Cdc24 (Scd1) localization at cell ends via negative feedback (Gulli *et al.*, 2000; Howell *et al.*,
194 2012; Wu and Lew, 2013; Kuo *et al.*, 2014; Wu *et al.*, 2015; Rapali *et al.*, 2017). In fission yeast
195 *pak1-ts* hypomorphic mutants, high amounts of Scd1 and active Cdc42 accumulate at only one
196 end causing the characteristic monopolar and wide phenotype (Verde *et al.*, 1998; Das *et al.*,
197 2012). We asked if Pak1 kinase also regulated Scd1 diffusion within the cytoplasm. To this end,
198 we investigated the rate of Scd1-mNG recruitment and diffusion using FRAP and FLIP in a
199 *pak1-ts* mutant background. We used FRAP to measure Scd1-mNG recruitment to cell ends in
200 *pak1-ts* mutants and found there is no significant difference between *pak1*$^{+}$ cells and *pak1-ts*
201 mutants (Fig. 4A, B, C). This suggests that the lack of Pak1 kinase on Scd1 does not
202 significantly impact Scd1-mNG recruitment to cell ends (Fig. 4A, B, C). Next, we used FLIP and
203 measured fluorescence loss at the cell ends to quantify if the lack of Pak1 kinase impacted
204 Scd1 diffusion. We find that Scd1-mNG intensity loss is significantly slower in *pak1-ts* mutants
205 when compared to *pak1*$^{+}$ cells (Fig. 4D). The half-life of fluorescence loss of Scd1-mNG in
206 *pak1*$^{+}$ cells is 74 seconds while that in *pak1-ts* mutants is 140 seconds (Fig. 4E). These data
207 suggest that in the absence of Pak1 kinase activity, Scd1-mNG diffusion is significantly delayed
208 and even slower than Scd1-2xGFP and Scd1-3xGFP. The mechanism of how Pak1-dependent
209 phosphorylation of Scd1 diffusion will be investigated further in future studies.

210

211 **The scaffold Scd2 shows slower diffusion dynamics compared to Scd1**

212 We asked if like Scd1, its scaffold Scd2 also diffused from one end of the cell to the
213 other with similar dynamics? It is possible that the dynamics of Scd2, the Scd1 scaffold, dictates
214 the rate of Scd1 diffusion to the sites of growth. To test this possibility, we compared the rates of
215 diffusion between Scd1-mNG and Scd2-GFP. We began by comparing the distribution of Scd1-
216 mNG within the cell to Scd2-GFP (Fig. 5A, B). We again see that Scd1-mNG has roughly 50%
217 of its intensity in the cytoplasm when compared to the cell ends. By contrast, Scd2-GFP only
218 shows about 25% of its intensity in the cytoplasm relative to the Scd2 intensity at the cell ends
219 (Fig. 5A, B, C). Moreover. While we see a consistent dip in Scd1 levels in the cytoplasm right
220 next to the end with increased levels, we do not such a dip for Scd2 near the ends (Fig. 5B, red
221 arrow).

222 Next, we performed FLIP on Scd1-mNG cells and Scd2-GFP cells to compare their rates
223 of exchange between the two halves of the cell (Fig. 5D). We find that like Scd1-mNG, Scd2-
224 GFP is also exchanged between the cytoplasm and cell ends. However, Scd1-mNG intensity is
225 rapidly lost from the cell end whereas Scd2-GFP loss is slower (Fig. 5D, E). The average half-
226 life of fluorescence intensity loss for Scd1-mNG is around 70 seconds on average whereas the
227 half-life of Scd2 loss is over 200 seconds (Fig. 5E, F). Together, these data suggest that while
228 Scd1 diffuses from one cell end to the other for bipolar Cdc42 activation, Scd2 diffusion is much
229 slower and thus likely not a factor in Cdc42 oscillatory dynamics. Indeed, the fluorescence
230 decay of Scd2-GFP at the opposite end is even slower than that Scd1-2xGFP and -3xGFP
231 (Fig.5H). Thus, Scd1 (99 kDa) has a higher ratio of cytoplasmic localization and is exchanged
232 rapidly between growing ends despite Scd2 (60 kDa) being the smaller and more abundant
233 protein. This further suggests mass is not the only factor that impacts diffusion and the intrinsic
234 properties of Scd1 facilitate its rapid diffusion.

235

236 **Conclusions**

237 We previously found that Pak1 removal via endocytosis is vital for Scd1 localization and
238 allows for the repeated cycle of Cdc42 activation at a cell end (Harrell *et al.*, 2024). Here we
239 show that Scd1 localizes to the growing cell ends via diffusion between those ends. Thus, Pak1
240 phosphorylation must facilitate adequate Scd1 turnover at cell ends such that there is enough
241 cytoplasmic Scd1 molecules to diffuse to the other end to drive Cdc42 activation between the
242 different sites of growth. Thus, we find yet another layer of self-regulation in this polarity system
243 where Scd1 diffusion within the cytoplasm activates Cdc42 and promotes bipolar growth.

244 FLIP analysis of Scd1-3xGFP shows that when the half-life is slowed to around 100 seconds or
245 more, most cells in the population are monopolar. This suggests Scd2 is exchanged less rapidly
246 while Scd1, with a half-life of 70 seconds, must be rapidly exchanged to promote proper
247 competition and bipolar growth. While we see differences in the diffusion rate of Scd1 and Scd2,
248 its rate of recruitment at the cell ends as determined by FRAP is similar (Harrell *et al.*, 2024). It
249 is possible the once Scd1 is available at an end via diffusion, local Scd2 at that end facilitates
250 Scd1 recruitment to the plasma membrane. In such a scenario, Scd2 diffusion between ends
251 would not be necessary for Cdc42 oscillatory dynamics. The finding that Scd2 diffusion is slower
252 than the diffusion of Scd1 suggests that this diffusion is not random and that the intrinsic
253 properties of the proteins impact their diffusion rates. Scd1 has a higher amount of intrinsically
254 disordered regions when compared to Scd2. While the functional significance of intrinsically
255 disordered regions remain to be fully understood, these regions may have roles in facilitating
256 Scd1 diffusion, possibly by making the protein more soluble when diffusing. The intrinsically
257 disordered regions or other properties of Scd1 may explain why simply increasing the mass
258 beyond 54.2kDa (-2xGFP and -3xGFP) alone does not further dampen Scd1 dynamics.

There is a consistent drop in cytoplasmic Scd1 intensity near the active growing end. More investigation is needed to test the significance of this pattern. It is possible that this is a region of active recruitment and turnover, so most Scd1 molecules that are within this region are rapidly recruited to the membrane of the growing cell end. Scd1 would need to be beyond a certain threshold of an active end to have a chance of diffusing to the opposite cell end. This threshold may be easier to overcome when an end is saturated and reaches its carrying capacity such that it can no longer accumulate more Scd1.

Scd1 diffusion appears to slow down in mutants of the *pak1* kinase. In Pak1 kinase mutants, Scd1 is not removed from the cell ends via negative feedback (Das *et al.*, 2012). In these cells Scd1 accumulates at only one cell end and the cells are monopolar. These mutants do show cytoplasmic Scd1 with similar recruitment rates at the growing cell end similar to that of *pak1*$^{+}$ cells. However, they display slower diffusion rates suggesting that Pak1 kinase may play a role in regulating Scd1 diffusion. Indeed, the half-life of fluorescence decay in *pak1-ts* mutants is even slower than that of Scd1-3xGFP. This further highlights how Scd1 diffusion is dependent on its intrinsic properties and not just on its mass.

Scd1 is recruited to the cell membrane in its dephosphorylated form (Das *et al.*, 2012). Given that our data show that Scd1 diffuses from one end of the cell to the next, it raises the possibility that a phosphatase is involved in this regulation where it dephosphorylates Scd1, thereby enabling membrane recruitment and Cdc42 activation. Such a kinase-phosphatase based regulatory system along with diffusion in the cytoplasm can allow the periodic redistribution of Scd1 at the cell ends to promote bipolar growth. Further investigations will define if similar diffusion dependent localization of Cdc42 GEFs also occur in animal cells to enable multipolar growth.

While the role for protein diffusion in the cytoplasm has not been clearly understood in biological systems, a recent report has shown that increasing cytoplasmic viscosity impairs protein diffusion in the cell and this can impact dynamic cellular processes (Molines *et al.*, 2022). Cytoplasmic viscosity impacts protein diffusion in both fission yeast cells as well as in animal cells. Thus, this may be a conserved form of regulation and further studies will define the mechanistic details of diffusion of Scd1 and other proteins in polarity control.

288 **MATERIALS AND METHODS**

289 **Strains and Cell Culture**

290 The *S. pombe* strains used in this study are listed in Table S1. All strains are isogenic to
291 the original strain PN567. Cells were cultured in yeast extract (YE) medium and grown
292 exponentially at 25°C unless specified otherwise. Standard techniques were used for genetic
293 manipulation and analysis (Moreno *et al.*, 1991). Cells were grown exponentially for at least three
294 rounds of eight generations each before imaging.

295

296 **Microscopy**

297 Imaging was performed at room temperature (23–25°C). We used a Nikon Ti2 Eclipse
298 wide-field microscope with a 100×/1.49 NA objective and an ORCA-FusionBT digital camera
299 (Hamamatsu Model: C15440-20UP Serial No: 500428). Images were acquired using Nikon NIS
300 Elements (Nikon). Fluorophores were excited with an AURA Light Engine system (Lumencor).

301 Microscopy was also performed with a 3i spinning disk confocal using a Zeiss
302 AxioObserver microscope with an integrated Yokogawa spinning disk (Yokogawa CSU-X1 A1
303 spinning disk scanner) and a 100×/1.49 NA objective. Images were acquired with a Teledyne
304 Photometrics Prime 95b back illuminated sCMOS camera (Serial No: A20D203014). Images
305 were acquired using SlideBook (3i Intelligent Imaging innovations).

306

307 **Acquiring and Quantifying Fluorescence Intensity**

308 Fluorescence intensity was measured using ImageJ software. All images were sum
309 projected and mean intensities were reported. Freehand ROIs were used to measure the signal
310 at the cell ends. For analysis of two ends of the same cell, cytoplasm with little or no signal was

311 used for background subtraction. For all other experiments, a region outside of the cell was
312 used for background subtraction. The mean intensity was measured and recorded after the
313 background subtractions.

314 For FLIP analysis, cells were imaged every 10 s for 10 minutes with 4% laser power at
315 488nm wavelength. Bleaching repeatedly occurs every 2$^{nd}$ timepoint (1 bleach every 20
316 seconds). The resulting FLIP data was fitted to a one-phase decay curve to indicate the time to
317 lose 50% of fluorescence at the opposite cell end for each cell in each experiment.

318 For FRAP analysis, cells were imaged every 250 ms for 30 s with 15% laser power at
319 488nm wavelength. Square 10 x 10 Pixel (1.1 × 1.1 μm) ROIs were used to target, bleach, and
320 measure the fluorescence intensity at half of one cell end as it was bleached and then allowed
321 to recover. The first nine time points were acquired before photobleaching and served as a
322 measurement of the initial fluorescence intensity. On the 10th time point, the acquisition was
323 halted momentarily and the region of interest was photobleached using three 4% laser power
324 bleach repetitions with a duration of 5 ms each (15 ms total). After the region of interest was
325 bleached, acquisition resumed at 250 ms intervals as the fluorescence intensity recovered. The
326 half-life of fluorescence recovery was quantified using SlideBook FRAP analysis software.

327 To quantify signal stability at the cell ends, cells were imaged every 30 s for 20 min. The
328 stability of the proteins was then quantified by measuring the difference in intensity between
329 each subsequent time point for the duration of the timelapse imaging. Populations that had
330 larger average variations of fluorescent intensity between each timepoint were more dynamic
331 and less stable than populations that had smaller variations between each timepoint.

332

333 **Statistical tests**

334 Statistical significance was computed with GraphPad Prism. When comparing two
335 conditions, Student's t-test was used (two-tailed, unequal variance). One-way ANOVA, followed
336 by Tukey's multiple comparison tests, was used to determine significance of experiments with
337 three or more conditions. SuperPlots (Lord *et al.*, 2020) were made using GraphPad Prism.
338

**Acknowledgements**

We thank Bret Judson and the Boston College Imaging Core for infrastructure and support. We thank Sophie Martin, and Fulvia Verde for providing strains. This work is supported by the National Institutes of Health grant R01GM136847 to M.D.

**Declaration of interests**

The authors declare no competing or financial interests.

347 **FIGURE LEGENDS**

348 **Figure 1. Scd1 is highly cytoplasmic and diffuses along the cytoplasm between cell ends.**
349 (A) Scd1-mNG localization in *for3*$^{+}$ cells compared to *for3*Δ mutants. Magenta rectangle indicates
350 the cell example shown in C. (B) Quantification of mean Scd1-mNG intensity at cell ends in the
351 indicated strains. (C) Averaged plot profile of end-to-end Scd1-mNG distribution along the long
352 axis of the cell in G2 cells (n=59). (D) The ratio of cytoplasmic intensity relative to intensity at the
353 cell ends (N=3, n=59). (E) Diagram illustrating fluorescence loss in photobleaching (FLIP). Top:
354 If there is exchange of protein between the cytoplasm and the opposite cell end, we will see loss
355 in fluorescence at the end. The fluorescence decay graphs will determine the rate of diffusion.
356 Bottom: If there is no exchange of protein between the two halves of the cell, we will not see loss
357 of fluorescence at the opposite cell end. (F) FLIP performed on Scd1-mNG expressing cell.
358 Magenta dotted outline indicates the bleached cell. Cyan asterisk shows the repeatedly bleached
359 region. Magenta arrow indicates when about 50% of the fluorescence is lost at the cell end. Blue
360 arrow indicates roughly when all signal is lost at the cell end. (G) FLIP experiments are pooled
361 and fitted to a one phase decay curve. (H) Quantification of the time to lose 50% of fluorescence
362 (half-life) of Scd1-mNG in FLIP experiments. Scale bar, 10 μm. n.s., not significant; P value,
363 *<0.05, Student's t test.

364

365 **Figure 2. Dampened Scd1 dynamics correlate with dampened Cdc42 activation. (A)**
366 Montage of CRIB-mCherry dynamics in Scd1-mNG cells and Scd1-3xGFP cells. **(B)**
367 Representative graphs of CRIB-mCherry dynamics in Scd1-mNG cells and Scd1-3xGFP cells.
368 **(C)** Quantification of the extent of Pak1-mEGFP fluctuations at the cell ends (N = 3, n ≥ 5 cells).
369 (**D)** Quantification of the percentage of monopolar cells observed in each culture. (N=3, n ≥ 10
370 cells). Scale bar, 10 μm. P value, *<0.05, **<0.005, ****<0.0001, Student's t test and one-way
371 ANOVA followed by Tukey's multiple comparison test.

372

373 **Figure 3. FLIP and FRAP analysis of Scd1 with additional mass. (A)** Scd1-mNG, -2xGFP,
374 and -3xGFP cells were subjected to FLIP and loss in fluorescence was pooled and fitted to a
375 one-phase decay curve (n≥15). **(B)** Comparison of the half-lives of fluorescence loss in Scd1-
376 mNG, -2xGFP, and -3xGFP cells (n≥15). **(C)** FRAP will be used to completely bleach half of one
377 cell end and we will quantify the rate of fluorescence recovery at this cell end. (**D)** Averaged
378 FRAP graphs for Scd1-mNG, -2xGFP and -3xGFP. (n≥13). **(E)** Quantification of the half-lives of
379 FRAP in cells expressing Scd1-mNG, -2xGFP, and -3xGFP. (n≥17). Scale bar, 10 µm. n.s., not
380 significant; P value, *<0.05, **<0.005, one-way ANOVA followed by Tukey's multiple comparison
381 test.
382
383 **Figure 4. Loss of *pak1* kinase decreases Scd1 diffusion rates. (**A) Montage of Scd1-mNG
384 FRAP in *pak1*$^{+}$ and *pak1-ts* cells. Magenta boxes indicate the half of the cell end that has been
385 photobleached. Magenta arrows show when half of the final fluorescence has recovered. Blue
386 arrows indicate when the fluorescence recovery plateaus. (B) Averaged fluorescence recovery
387 graphs of Scd1-mNG FRAP in *pak1*$^{+}$ and *pak1-ts* cells. (C) Half-life of fluorescence recovery in
388 *pak1*$^{+}$ and *pak1-ts* cells (n≥16). (D) FLIP of Scd1-mNG in *pak1*$^{+}$ and *pak1-ts* cells cells. The
389 fluorescence loss at the cell ends was pooled and fitted to a one-phase decay (n≥10). (E)
390 Quantification of Scd1-mNG loss at the cell ends of *pak1*$^{+}$ and *pak1-ts* cells (n≥10). Scale bar,
391 10 µm. n.s., not significant; P value, *<0.05, Student's t test.
392
393 **Figure 5. FLIP reveals that Scd1 diffuses between the cytoplasm and cell ends more**
394 **rapidly than Scd2.** (A) Cellular localization of Scd1-mNG and Scd2-GFP. (B) End-to-end
395 fluorescence intensity profiles of Scd1-mNG and Scd2-GFP along the long axis of the cell (n=
396 60). (C) Ratio of cytoplasmic intensity relative to the intensity at the cell ends for Scd1-mNG
397 compared to Scd2-GFP (N=3, n = 20 cells per replicate). (D) Montages of FLIP in Scd1-mNG
398 and Scd2-GFP. Magenta dotted line indicates the bleached cell. Cyan asterisk shows the

399 repeatedly bleached region. Magenta arrow indicates roughly when 50% of fluorescence is lost
400 at the cell end. Blue arrow indicates roughly when all signal is lost at the cell end. (E) Pooled
401 fluorescence loss for Scd1-mNG and Scd2-GFP fitted to a one phase decay curve (n ≥16). (F)
402 Half-lives of fluorescence loss in Scd1-mNG compared to Scd2-GFP (n ≥16). (H) One phase
403 decay curve of fluorescence loss of Scd2-GFP data repurposed from Figure 4 and Scd1-2xGFP
404 and -3xGFP data repurposed from Figure 2 (n≥15). Scale bar, 10 μm. n.s., not significant; P
405 value, **<0.005, ***<0.0009, Student's t test.

406 **REFERENCES**


407 Axelrod, D., Koppel, D.E., Schlessinger, J., Elson, E., and Webb, W.W. (1976). Mobility
408 measurement by analysis of fluorescence photobleaching recovery kinetics. Biophys J *16*,
409 1055-1069.

410 Butty, A.C. (2002). A positive feedback loop stabilizes the guanine-nucleotide exchange factor
411 Cdc24 at sites of polarization. The EMBO Journal *21*, 1565-1576.

412 Butty, A.C., Perrinjaquet, N., Petit, A., Jaquenoud, M., Segall, J.E., Hofmann, K., Zwahlen, C.,
413 and Peter, M. (2002). A positive feedback loop stabilizes the guanine-nucleotide exchange
414 factor Cdc24 at sites of polarization. Embo j *21*, 1565-1576.

415 Chang, E., Bartholomeusz, G., Pimental, R., Chen, J., Lai, H., Wang, L.-H.L., Yang, P., and
416 Marcus, S. (1999). Direct Binding and In Vivo Regulation of the Fission Yeast p21-Activated
417 Kinase Shk1 by the SH3 Domain Protein Scd2. Molecular and Cellular Biology *19*, 8066-8074.

418 Chang, E.C., Barr, M., Wang, Y., Jung, V., Xu, H.P., and Wigler, M.H. (1994). Cooperative
419 interaction of S. pombe proteins required for mating and morphogenesis. Cell *79*, 131-141.

420 Cole, N.B., Smith, C.L., Sciaky, N., Terasaki, M., Edidin, M., and Lippincott-Schwartz, J. (1996).
421 Diffusional mobility of Golgi proteins in membranes of living cells. Science *273*, 797-801.

422 Coll, P.M., Trillo, Y., Ametzazurra, A., and Perez, P. (2003). Gef1p, a new guanine nucleotide
423 exchange factor for Cdc42p, regulates polarity in Schizosaccharomyces pombe. Mol Biol Cell
424 *14*, 313-323.

425 Das, M., Drake, T., Wiley, D.J., Buchwald, P., Vavylonis, D., and Verde, F. (2012). Oscillatory
426 Dynamics of Cdc42 GTPase in the Control of Polarized Growth. Science *337*, 239-243.

427 Das, M., and Verde, F. (2013). Role of Cdc42 dynamics in the control of fission yeast cell
428 polarization. Biochemical Society transactions *41*, 1745-1749.

429 Feierbach, B., and Chang, F. (2001). Roles of the fission yeast formin for3p in cell polarity, actin
430 cable formation and symmetric cell division. Curr Biol *11*, 1656-1665.

431 Gulli, M.P., Jaquenoud, M., Shimada, Y., Niederhäuser, G., Wiget, P., and Peter, M. (2000).
432 Phosphorylation of the Cdc42 exchange factor Cdc24 by the PAK-like kinase Cla4 may regulate
433 polarized growth in yeast. Mol Cell *6*, 1155-1167.

434 Hall, A. (1990). The cellular functions of small GTP-binding proteins. Science *249*, 635-640.

435 Harrell, M.A., Liu, Z., Campbell, B.F., Chinsen, O., Hong, T., and Das, M. (2024). Arp2/3-
436 dependent endocytosis ensures Cdc42 oscillations by removing Pak1-mediated negative
437 feedback. The Journal of cell biology *223*.

438 Hercyk, B.S., Rich-Robinson, J., Mitoubsi, A.S., Harrell, M.A., and Das, M.E. (2019a). A novel
439 interplay between GEFs orchestrates Cdc42 activity during cell polarity and cytokinesis. Journal
440 of Cell Science *132*, jcs236018.

441 Hercyk, B.S., Rich-Robinson, J., Mitoubsi, A.S., Harrell, M.A., and Das, M.E. (2019b). A novel
442 interplay between GEFs orchestrates Cdc42 activity during cell polarity and cytokinesis in
443 fission yeast. Journal of cell science *132*.

444 Howell, A.S., Jin, M., Wu, C.F., Zyla, T.R., Elston, T.C., and Lew, D.J. (2012). Negative feedback
445 enhances robustness in the yeast polarity establishment circuit. Cell *149*, 322-333.

446 Jacobson, K., Derzko, Z., Wu, E.-S., Hou, Y., and Poste, G. (1976). Measurement of the lateral
447 mobility of cell surface components in single living cells by fluorescence recovery after
448 photobleaching. Journal of Supramolecular Structure *5*, 565-576.

449 Johnson, D.I. (1999). Cdc42: An essential Rho-type GTPase controlling eukaryotic cell polarity.
450 Microbiol Mol Biol Rev *63*, 54-105.

451 Kozubowski, L., Saito, K., Johnson, J.M., Howell, A.S., Zyla, T.R., and Lew, D.J. (2008).
452 Symmetry-Breaking Polarization Driven by a Cdc42p GEF-PAK Complex. Current Biology *18*,
453 1719-1726.

454 Kuo, C.C., Savage, N.S., Chen, H., Wu, C.F., Zyla, T.R., and Lew, D.J. (2014). Inhibitory GEF
455 phosphorylation provides negative feedback in the yeast polarity circuit. Current biology : CB *24*,
456 753-759.

457 Lord, S.J., Velle, K.B., Mullins, R.D., and Fritz-Laylin, L.K. (2020). SuperPlots: Communicating
458 reproducibility and variability in cell biology. J Cell Biol *219*.

459 Martin, S.G., and Chang, F. (2006). Dynamics of the formin for3p in actin cable assembly. Curr
460 Biol *16*, 1161-1170.

461 Matsuyama, A., Arai, R., Yashiroda, Y., Shirai, A., Kamata, A., Sekido, S., Kobayashi, Y.,
462 Hashimoto, A., Hamamoto, M., Hiraoka, Y., Horinouchi, S., and Yoshida, M. (2006). ORFeome
463 cloning and global analysis of protein localization in the fission yeast Schizosaccharomyces
464 pombe. Nature Biotechnology *24*, 841-847.

465 Miller, P.J., and Johnson, D.I. (1994). Cdc42p GTPase Is Involved in Controlling Polarized Cell
466 Growth in Schizosaccharomyces pombe. Molecular and Cellular Biology *14*, 1075-1083.

467 Molines, A.T., Lemiere, J., Gazzola, M., Steinmark, I.E., Edrington, C.H., Hsu, C.T., Real-
468 Calderon, P., Suhling, K., Goshima, G., Holt, L.J., Thery, M., Brouhard, G.J., and Chang, F.
469 (2022). Physical properties of the cytoplasm modulate the rates of microtubule polymerization
470 and depolymerization. Developmental cell *57*, 466-479 e466.

471 Moreno, S., Klar, A., and Nurse, P. (1991). Molecular genetic analysis of fission yeast
472 Schizosaccharomyces pombe. Methods Enzymol *194*, 795-823.

473 Murray, J.M., and Johnson, D.I. (2001). The Cdc42p GTPase and Its Regulators Nrf1p and
474 Scd1p Are Involved in Endocytic Trafficking in the Fission YeastSchizosaccharomyces pombe *.
475 Journal of Biological Chemistry *276*, 3004-3009.

476 Nakano, K., Imai, J., Arai, R., Toh, E.A., Matsui, Y., and Mabuchi, I. (2002). The small GTPase
477 Rho3 and the diaphanous/formin For3 function in polarized cell growth in fission yeast. Journal
478 of cell science *115*, 4629-4639.

479 Nobes, C.D., and Hall, A. (1999). Rho GTPases control polarity, protrusion, and adhesion during
480 cell movement. J Cell Biol *144*, 1235-1244.

481 Poo, M., and Cone, R.A. (1974). Lateral diffusion of rhodopsin in the photoreceptor membrane.
482 Nature *247*, 438-441.

483 Rapali, P., Mitteau, R., Braun, C., Massoni-Laporte, A., Unlu, C., Bataille, L., Arramon, F.S.,
484 Gygi, S.P., and McCusker, D. (2017). Scaffold-mediated gating of Cdc42 signalling flux. Elife *6*.

485 Rossman, K.L., Der, C.J., and Sondek, J. (2005). GEF means go: turning on RHO GTPases
486 with guanine nucleotide-exchange factors. Nature Reviews Molecular Cell Biology *6*, 167-180.

487 Salat-Canela, C., Carmona, M., Martin-Garcia, R., Perez, P., Ayte, J., and Hidalgo, E. (2021).
488 Stress-dependent inhibition of polarized cell growth through unbalancing the GEF/GAP
489 regulation of Cdc42. Cell reports *37*, 109951.

490 Sawin, K.E., and Nurse, P. (1998). Regulation of cell polarity by microtubules in fission yeast. J
491 Cell Biol *142*, 457-471.

492 Scheffzek, K., and Ahmadian, M.R. (2005). GTPase activating proteins: structural and functional
493 insights 18 years after discovery. Cellular and Molecular Life Sciences CMLS *62*, 3014-3038.

494 Shcheprova, Z., Baldi, S., Frei, S.B., Gonnet, G., and Barral, Y. (2008). A mechanism for
495 asymmetric segregation of age during yeast budding. Nature *454*, 728-734.

496 Stengel, K., and Zheng, Y. (2011). Cdc42 in oncogenic transformation, invasion, and
497 tumorigenesis. Cellular Signalling *23*, 1415-1423.

498 Verde, F., Wiley, D.J., and Nurse, P. (1998). Fission yeast orb6, a ser/thr protein kinase related
499 to mammalian rho kinase and myotonic dystrophy kinase, is required for maintenance of cell
500 polarity and coordinates cell morphogenesis with the cell cycle. Proceedings of the National
501 Academy of Sciences of the United States of America *95*, 7526-7531.

502 Verkman, A.S. (2002). Solute and macromolecule diffusion in cellular aqueous compartments.
503 Trends in Biochemical Sciences *27*, 27-33.

504 Wei, B., Hercyk, B.S., Mattson, N., Mohammadi, A., Rich, J., DeBruyne, E., Clark, M.M., and
505 Das, M. (2016). Unique Spatiotemporal Activation Pattern of Cdc42 by Gef1 and Scd1 Promotes
506 Different Events during Cytokinesis. Molecular biology of the cell *27*, 1235-1245.

507 Wheatley, E., and Rittinger, K. (2005). Interactions between Cdc42 and the scaffold protein
508 Scd2: requirement of SH3 domains for GTPase binding. The Biochemical journal *388*, 177-184.

509 White, J., and Stelzer, E. (1999). Photobleaching GFP reveals protein dynamics inside live cells.
510 Trends in Cell Biology *9*, 61-65.

511 Wu, C.F., Chiou, J.G., Minakova, M., Woods, B., Tsygankov, D., Zyla, T.R., Savage, N.S.,
512 Elston, T.C., and Lew, D.J. (2015). Role of competition between polarity sites in establishing a
513 unique front. Elife *4*.

514 Wu, C.F., and Lew, D.J. (2013). Beyond symmetry-breaking: competition and negative feedback
515 in GTPase regulation. Trends in cell biology *23*, 476-483.

516 Zhang, B., Zhang, Y., Collins, C.C., Johnson, D.I., and Zheng, Y. (1999). A built-in arginine finger
517 triggers the self-stimulatory GTPase-activating activity of rho family GTPases. J Biol Chem *274*,
518 2609-2612.

519

# Figure 1

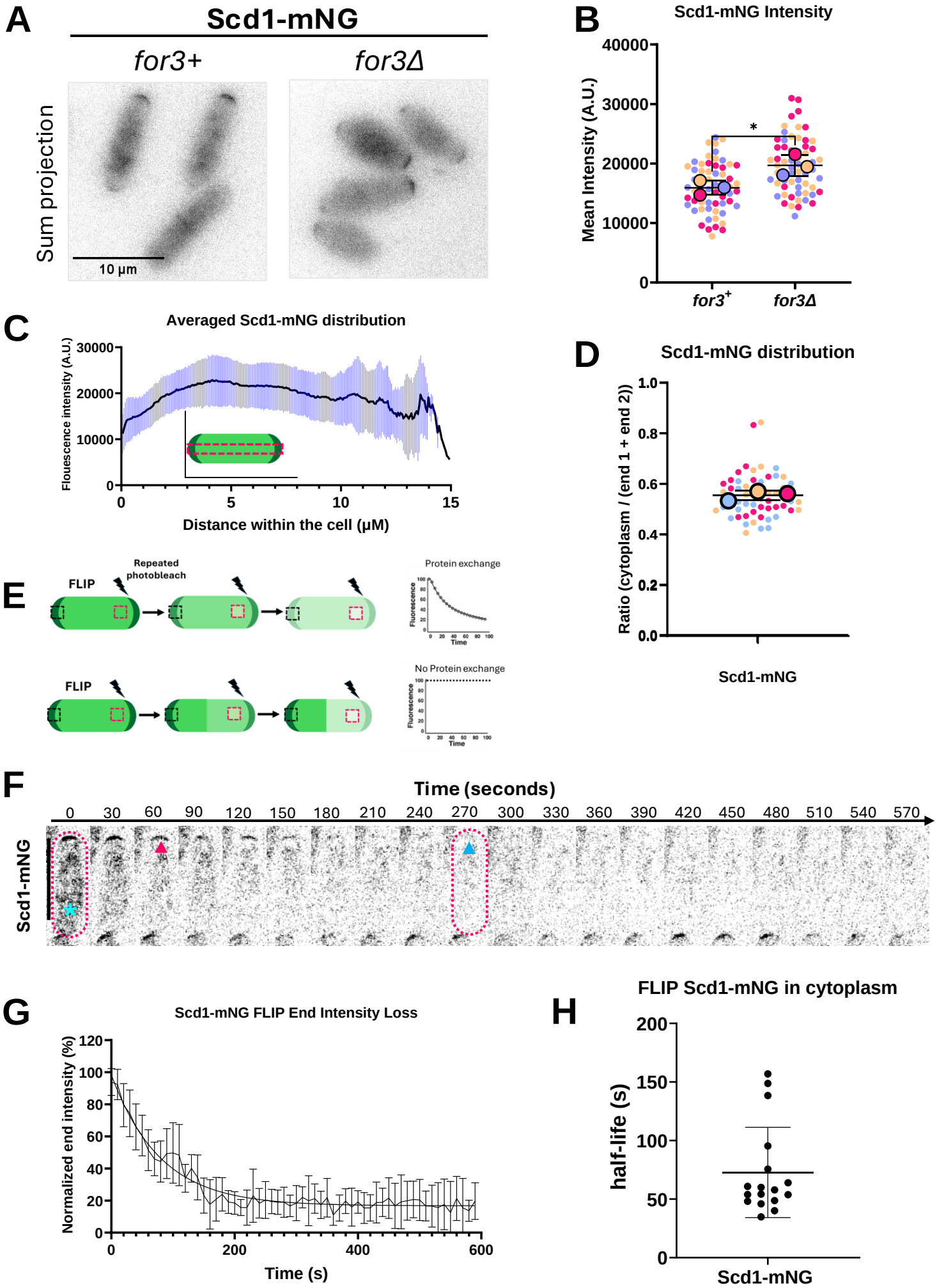
A
Scd1-mNG
for3+
for3Δ
Sum projection
10 µm
B
Scd1-mNG Intensity
Mean Intensity (A.U.)
40000
30000
20000
10000
0
*
for3+
for3Δ
C
Averaged Scd1-mNG distribution
Flouescence intensity (A.U.)
30000
20000
10000
0
0
5
10
15
Distance within the cell (µM)
D
Scd1-mNG distribution
Ratio (cytoplasm / (end 1 + end 2))
1.0
0.8
0.6
0.4
0.2
0.0
Scd1-mNG
E
FLIP
Repeated photobleach
Protein exchange
Fluorescence
Time
FLIP
No Protein exchange
Fluorescence
Time
F
Time (seconds)
0 30 60 90 120 150 180 210 240 270 300 330 360 390 420 450 480 510 540 570
Scd1-mNG
G
Scd1-mNG FLIP End Intensity Loss
Normalized end intensity (%)
120
100
80
60
40
20
0
0
200
400
600
Time (s)
H
FLIP Scd1-mNG in cytoplasm
half-life (s)
200
150
100
50
0
Scd1-mNG

# Figure 2

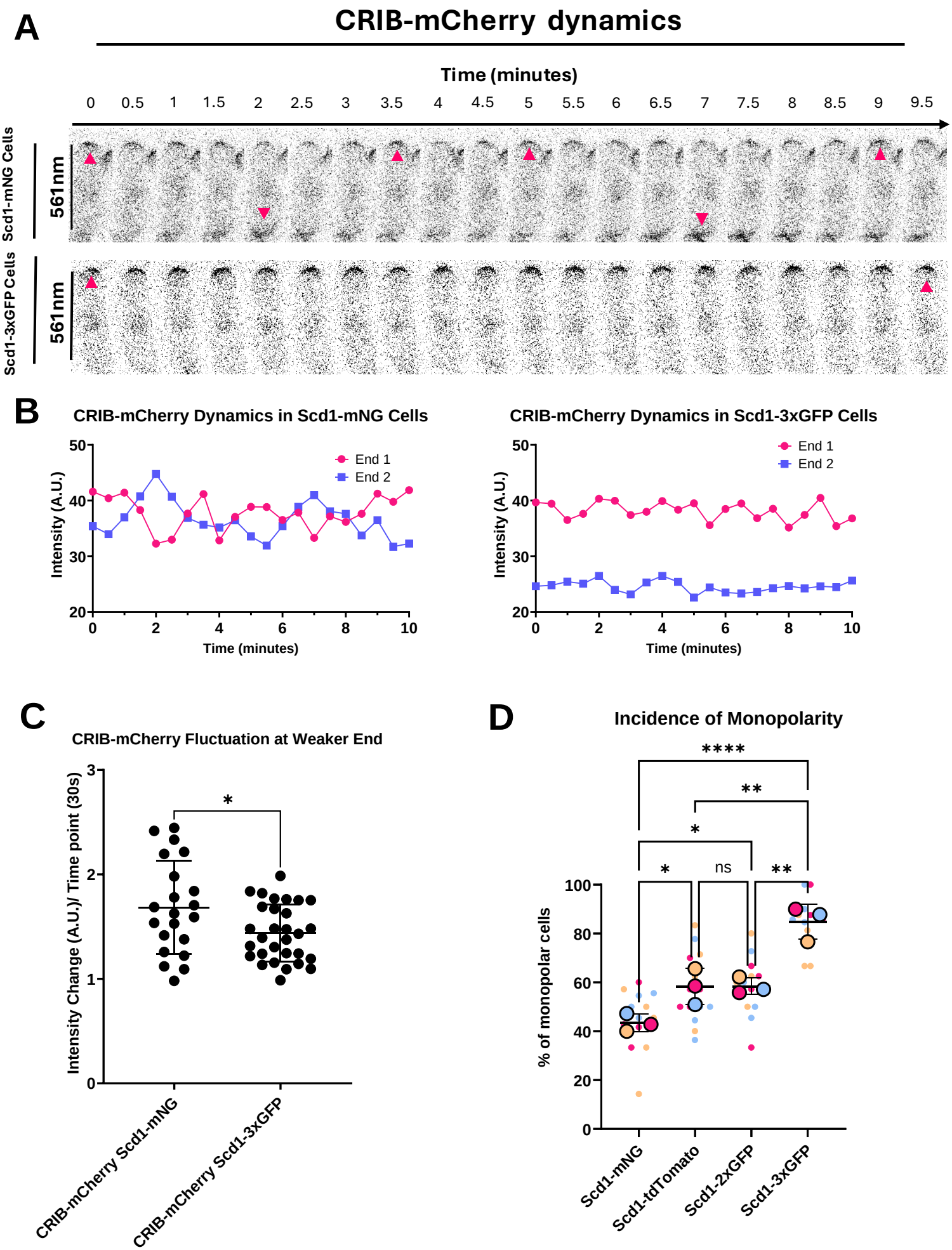
A
CRIB-mCherry dynamics
Time (minutes)
0 0.5 1 1.5 2 2.5 3 3.5 4 4.5 5 5.5 6 6.5 7 7.5 8 8.5 9 9.5
Scd1-mNG Cells
561 nm
Scd1-3xGFP Cells
561 nm
B
CRIB-mCherry Dynamics in Scd1-mNG Cells
CRIB-mCherry Dynamics in Scd1-3xGFP Cells
End 1
End 2
Intensity (A.U.)
Time (minutes)
C
CRIB-mCherry Fluctuation at Weaker End
Intensity Change (A.U.)/ Time point (30s)
*
CRIB-mCherry Scd1-mNG
CRIB-mCherry Scd1-3xGFP
D
Incidence of Monopolarity
% of monopolar cells
****
**
*
ns
Scd1-mNG
Scd1-tdTomato
Scd1-2xGFP
Scd1-3xGFP

# Figure 3

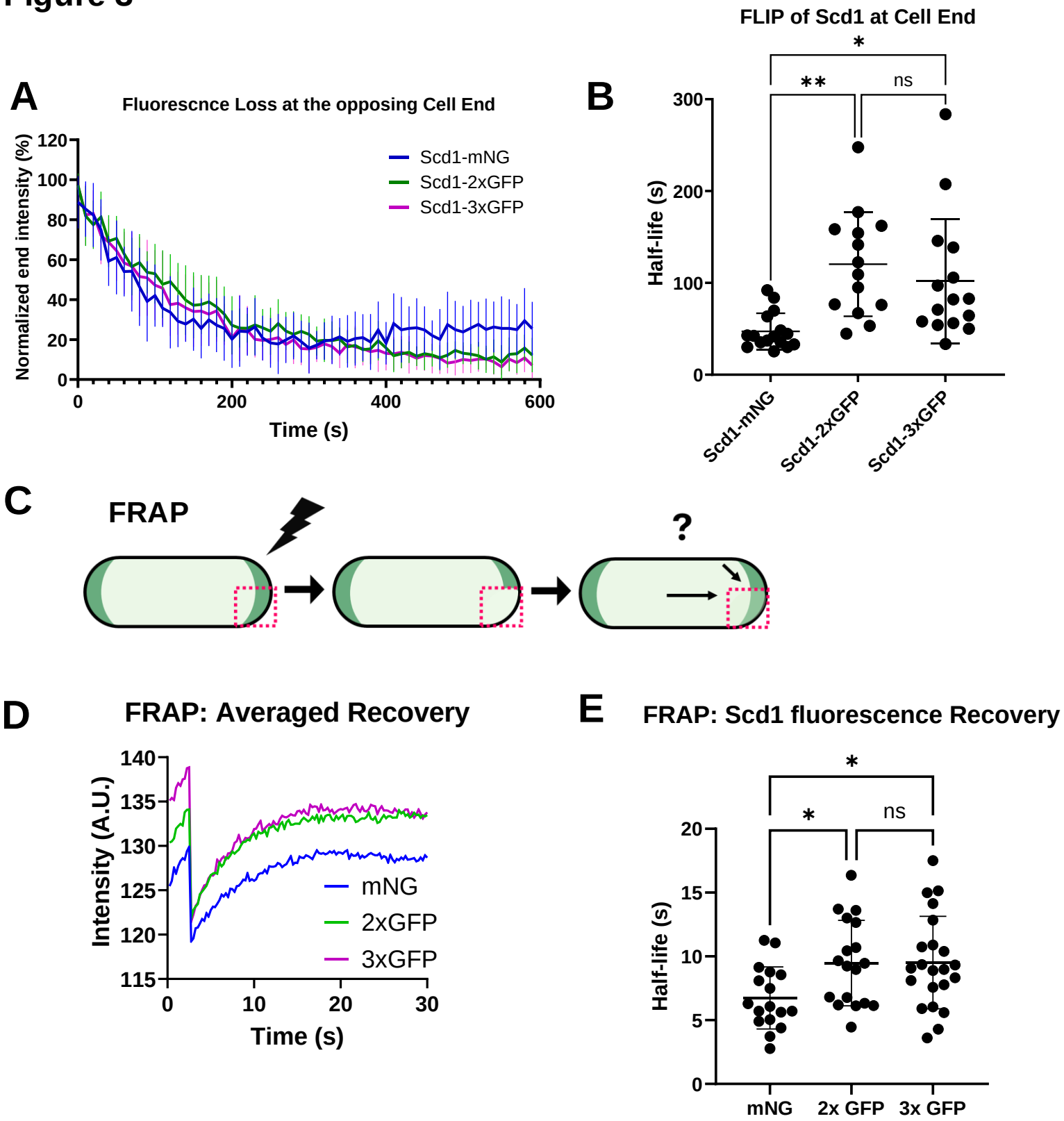
A
Fluorescnce Loss at the opposing Cell End
Normalized end intensity (%)
Time (s)
Scd1-mNG
Scd1-2xGFP
Scd1-3xGFP
B
FLIP of Scd1 at Cell End
Half-life (s)
*
**
ns
Scd1-mNG
Scd1-2xGFP
Scd1-3xGFP
C
FRAP
?
D
FRAP: Averaged Recovery
Intensity (A.U.)
Time (s)
mNG
2xGFP
3xGFP
E
FRAP: Scd1 fluorescence Recovery
Half-life (s)
*
*
ns
mNG
2x GFP
3x GFP

# Figure 4

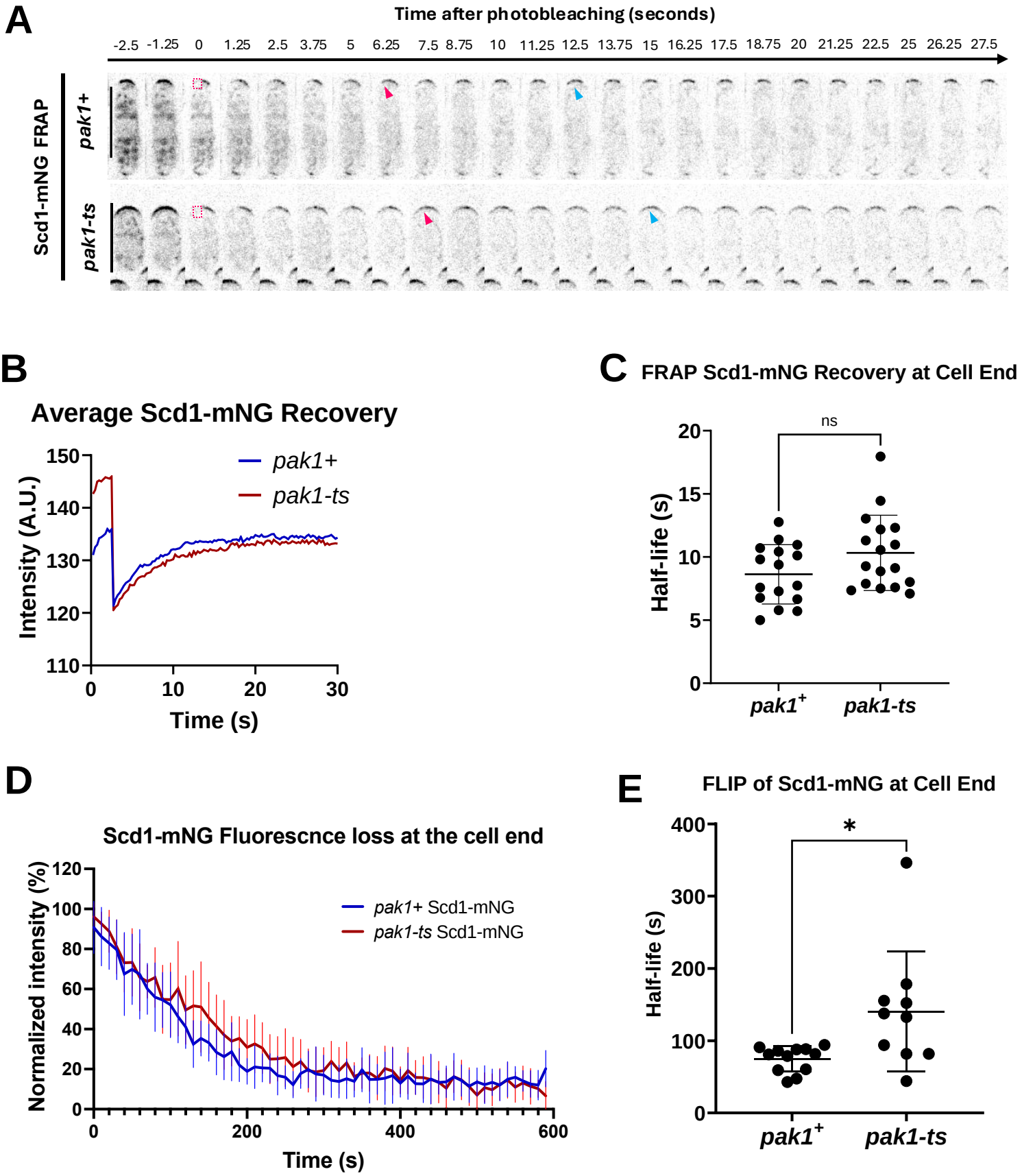
A
Time after photobleaching (seconds)
-2.5 -1.25 0 1.25 2.5 3.75 5 6.25 7.5 8.75 10 11.25 12.5 13.75 15 16.25 17.5 18.75 20 21.25 22.5 25 26.25 27.5
Scd1-mNG FRAP
pak1+
pak1-ts
B
Average Scd1-mNG Recovery
Intensity (A.U.)
150
140
130
120
110
0
10
20
30
Time (s)
pak1+
pak1-ts
C
FRAP Scd1-mNG Recovery at Cell End
ns
Half-life (s)
20
15
10
5
0
pak1+
pak1-ts
D
Scd1-mNG Fluorescnce loss at the cell end
Normalized intensity (%)
120
100
80
60
40
20
0
0
200
400
600
Time (s)
pak1+ Scd1-mNG
pak1-ts Scd1-mNG
E
FLIP of Scd1-mNG at Cell End
*
Half-life (s)
400
300
200
100
0
pak1+
pak1-ts

# Figure 5

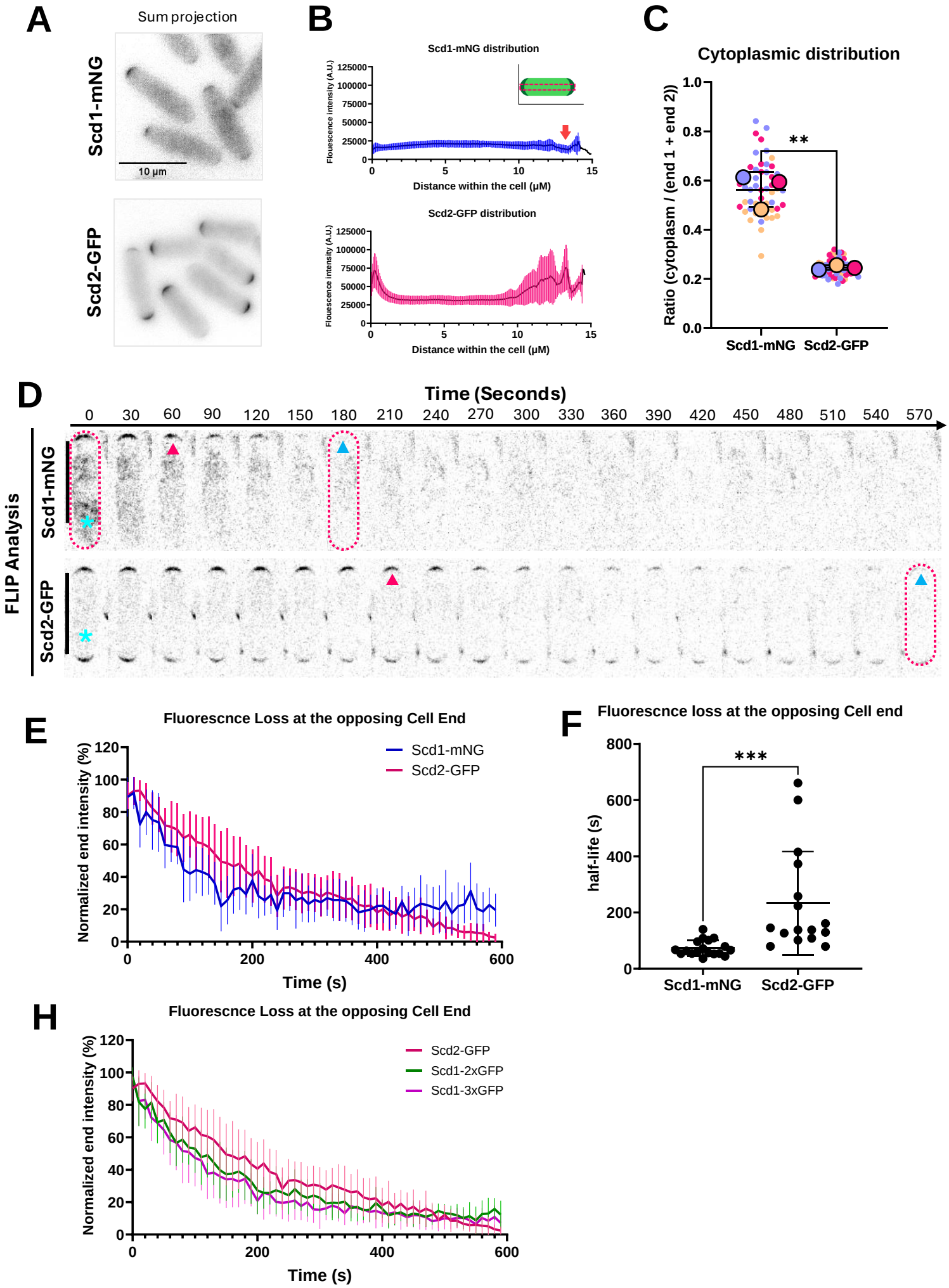
A
Sum projection
Scd1-mNG
Scd2-GFP
10 µm
B
Scd1-mNG distribution
Flouescence intensity (A.U.)
Distance within the cell (µM)
Scd2-GFP distribution
C
Cytoplasmic distribution
Ratio (cytoplasm / (end 1 + end 2))
**
Scd1-mNG
Scd2-GFP
D
Time (Seconds)
FLIP Analysis
Scd1-mNG
Scd2-GFP
E
Fluorescnce Loss at the opposing Cell End
Normalized end intensity (%)
Time (s)
Scd1-mNG
Scd2-GFP
F
Fluorescnce loss at the opposing Cell end
half-life (s)
***
Scd1-mNG
Scd2-GFP
H
Fluorescnce Loss at the opposing Cell End
Normalized end intensity (%)
Time (s)
Scd2-GFP
Scd1-2xGFP
Scd1-3xGFP